Staphylococcal Complement Inhibitor: Structure and Active Sites[1]

Suzan H. M. Rooijakkers,[2,3]* Fin J. Milder,[2†] Bart W. Bardoel,* Maartje Ruyken,* Jos A. G. van Strijp,* and Piet Gros[†]

The pathogenic bacterium *Staphylococcus aureus* counteracts the host immune defense by excretion of the 85 residue staphylococcal complement inhibitor (SCIN). SCIN inhibits the central complement convertases; thereby, it reduces phagocytosis following opsonization and efficiently blocks all downstream effector functions. In this study, we present the crystal structure of SCIN at 1.8 Å resolution and the identification of its active site. Functional characterization of structure based chimeric proteins, consisting of SCIN and the structurally but nonfunctional homologue open reading frame-D, indicate an 18-residue segment (Leu-31—Gly-48) crucial for SCIN activity. In all complement activation pathways, chimeras lacking these SCIN residues completely fail to inhibit production of the potent mediator of inflammation C5a. Inhibition of alternative pathway-mediated opsonization (C3b deposition) and formation of the lytic membrane attack complex (C5b-9 deposition) are strongly reduced for these chimeras as well. For inhibition of the classical/lectin pathway-mediated C3b and C5b-9 deposition, the same residues are critical although additional sites are involved. These chimeras also display reduced capacity to stabilize the C3 convertases of both the alternative and the classical/lectin pathway indicating the stabilizing effect is pivotal for the complement inhibitory activity of SCIN. Because SCIN specifically and efficiently inhibits complement, it has a high potential in anti-inflammatory therapy. Our data are a first step toward the development of a second generation molecule suitable for such therapeutic complement intervention. ***The Journal of Immunology,*** **2007, 179: 2989–2998.**

The complement system fulfills a critical role in our host defense against invading pathogens. As a key part of the innate immune system complement activation triggers acute inflammatory and cytolytic reactions but also participates in regulation of adaptive immunity (1–3). In contrast, unregulated complement activation is related to many unwanted inflammatory reactions associated with various acute and chronic inflammatory diseases (4, 5). The complement system is activated via two specific recognition pathways, the classical pathway (CP)[4] and lectin pathway (LP), that are amplified by the alternative pathway (AP) (6). All three pathways converge to the formation of an active protease complex on the pathogenic surface, the C3 convertase. The CP and LP convertases are formed when a C4b molecule covalently binds to the cell surface and is recognized by C2. Binding and subsequent cleavage of C2 results in the active convertase C4b2a. The AP convertase is formed in a similar manner by the proteins C3b and B, which are homologous to C4b and C2, respectively. Both bimolecular complexes (C3bBb and C4b2a) have a short lifetime ($t_{1/2}$ of 1–2 min) and their dissociation is irreversible (7). The C3 convertases cleave large amounts of complement protein C3 into C3a and C3b, thus, providing amplification. Convertase action results in labeling of Ags with a large number of C3b molecules and their inactive derivative iC3b (8–10). This so-called opsonization is essential for effective phagocytic uptake via complement receptors (11, 12). Furthermore, high local concentrations of C3b induce formation of C5 convertases (13). Cleavage of C5 by these convertases results in the release of C5a, an important chemoattractant, and C5b, the initiator of the membrane attack complexes (C5b-9) that directly lyses Gram-negative bacteria.

A bacterium must counteract immune responses to survive within its host. Increasing evidence suggests that the human pathogen *Staphylococcus aureus* is very successful in evading the innate immune defenses (14, 15). *S. aureus* blocks host defenses mainly by excretion of small molecules that inhibit several steps of the immune response. Neutrophil responses are inhibited by staphylococcal superantigen like (SSL)5 and the chemotaxis inhibitory protein of *S. aureus* (CHIPS) (16–18). SSL5 prevents neutrophil adhesion to the endothelial lining by binding P-selectin glycoprotein ligand 1, whereas CHIPS blocks neutrophil activation and chemotaxis by binding the C5aR and the formylated peptide receptor. Complement modulation was described for extracellular fibrinogen-binding protein (Efb) that binds C3 (fragments) and SSL7 that binds to C5 (19, 20).

Recently, we discovered a highly specific and unique complement modulator termed staphylococcal complement inhibitor (SCIN). SCIN is a 9.8 kDa protein excreted by *S. aureus* that

*Medical Microbiology, University Medical Center Utrecht, The Netherlands; and †Crystal and Structural Chemistry, Bijvoet Center for Biomolecular Research, Faculty of Science, Utrecht University, The Netherlands

Received for publication April 2, 2007. Accepted for publication June 15, 2007.

The costs of publication of this article were defrayed in part by the payment of page charges. This article must therefore be hereby marked *advertisement* in accordance with 18 U.S.C. Section 1734 solely to indicate this fact.

[1] This work was supported by grants from: Netherlands Organization for Scientific Research-VENI (916-76-037), a "Pionier" Programme Grant (to P.G.) of the Council for Chemical Sciences of Netherlands Organization for Scientific Research and Netherlands Genomics Initiative-Horizon (050-71-028).

[2] S.H.M.R. and F.J.M. contributed equally to this work.

[3] Address correspondence and reprint requests to Dr. Suzan H. M. Rooijakkers, Medical Microbiology, University Medical Center Utrecht, Room G04.614, Heidelberglaan 100, Utrecht, The Netherlands. E-mail address: s.h.m.rooijakkers@umcutrecht.nl

[4] Abbreviations used in this paper: CP, classical pathway; LP, lectin pathway; AP, alternative pathway; SSL, staphylococcal superantigen like; CHIPS, chemotaxis inhibitory protein of *S. aureus*; Efb, extracellular fibrinogen-binding protein; SCIN, staphylococcal complement inhibitor; MAD, multiwavelength anomalous dispersion; His, histidine; RCA, regulators of complement activation; Efb-C, C3-binding domain of Efb.

Table I. *Primers used in this study*

Protein	Primer Name	Primer Sequence[a]
SCIN	SCIN For	5′-GAGCACAAGCTTGCCAACATCG-3′
	SCIN Rev	5′-GGAATTCCTTAATATTTACTTTTT-3′
SCIN-B	SCIN-B For	5′-GAGTAGTCTGGACAAATATTTA-3′
	SCIN-B Rev	5′-GGAATTCCTTATCTATTTATAA-3′
SCIN-C	SCIN-C For	5′-GAGTAGTAAGAAAGACTATAT-3′
	SCIN-C Rev	5′-GGAATTCCTTATCTATTTATAATTTCA-3′
ORF-D	ORF-D For	5′-GAGCAAATCTGAAACTACATCACAT-3′
	ORF-D Rev	5′-GGAATTCCTTAATTGTTTTGTGAATGC-3′
CH-N	CH-N Rev	5′-AACGATTTTAATTCATTAGCTAACTTTTGATGTTGATACGTATGTGA-3′
	CH-N For	5′-CTACATCACATACGTATCAACATCAAAAGTTAGCTAATGAATTAAAATC-3′
CH-C	CH-C Rev	5′-GGAATTCCTTAATTGTTTTGACTTTTTAGTGCTTCGTCAAT-3′
CH-α1N	CH-$\alpha1_N$ Rev	5′-CAGTAGCTAATTCATTAACATTTAGGTTTGCTATTAATTCATGTA-3′
	CH-$\alpha1_N$ For	5′-TCAATTACATGAATTAATAGCAAACCTAAATGTTAATGAATTAGC-3′
CH-α1C	CH-$\alpha1_C$ Rev	5′-GGTACGATAATTTATTTAAGTCAGTTTCATCTAATAACGATTTTA-3′
	CH-$\alpha1_C$ For	5′-TGAATTAAAATCGTTATTAGATGAAACTGACTTAAATAAAT-3′
	CH-$\alpha1_C$ RevI	5′-TTATAGTTCGCTTATAATAAGTGTTTAAATTTAGGTACG-3′
	CH-$\alpha1_C$ ForI	5′-AAATAAATTATCGTACCTAAATTTAAACACTTATTATAAGCGAAC-3′
CH-α2N	CH-$\alpha2_N$ Rev	5′-AAATACGCGTTTTTGAAACGCATCTAAACTTCCAGTAGCTAATT-3′
	CH-$\alpha2_N$ For	5′-TAATGAATTAGCTACTGGAAGTTTAGATGCGTTTCAAAAA-3′
	CH-$\alpha2_N$ RevI	5′-ACTTAAGAGCATACATTGCTTTTAGGTGCGCAGCTAAAATATCG-3′
	CH-$\alpha2_N$ ForI	5′-AAAACGCGATATTTTAGCTGCGCACCTAAAAGCAATGTATGCTCT-3′
CH-α2C	CH-$\alpha2_C$ Rev	5′-TGCGTATAGCGGATTTTGCAATATAACCTGAAATTTTTATAGTTC-3′
	CH-$\alpha2_C$ For	5′-TAAGCGAACTATAAAAATTTCAGGTTATATTGCAAAATC-3′
	CH-$\alpha2_C$ RevI	5′-TTGCTTCTGACATTTTCTTAAAGTCTTTAGTGCGTATAG-3′
	CH-$\alpha2_C$ ForI	5′-TGCAAAATCCGCTATACGCACTAAAGACTTTAAGAAAATGTCAGA-3′
CH-α3N	CH-$\alpha3_N$ Rev	5′-TCGCTTTAGTCATTTGATCCAAATTTTTTGACTTAAGAGCATACA-3′
	CH-$\alpha3_N$ For	5′-AGCAATGTATGCTCTTAAGTCAAAAAATTTGGATCAAATGACTAA-3′
	CH-$\alpha3_N$ RevI	5′-GTGCTTCGTCAATTTCGTTATAAATACTTTCTAATCTTTGTTTCG-3′
	CH-$\alpha3_N$ ForI	5′-TAAAGCGAAACAAAGATTAGAAAGTATTTATAACGAAATTGACGA-3′
CH-α3C	CH-$\alpha3_C$ Rev	5′-AAGGGTTAGAAATTGAATTGTAAATCTTTTGAAGTTGATATTTTG-3′
	CH-$\alpha3_C$ For	5′-AGAAGCAAAATATCAACTTCAAAAGATTTACAATTCAATTTCTAA-3′
CH-α1CA	CH-$\alpha1_{CA}$ Rev	5′-TTTATTTAAGTCAGTTTCATCTAATAACGATTTTAATTC-3′
	CH-$\alpha1_{CA}$ For	5′-ACTGACTTAAATAAATTAGCTACTGGAAGTTTAAACACT-3′
CH-α1CB	CH-$\alpha1_{CB}$ Rev	5′-TAAATTTAGGTACGATAATTCATTAACATTTAGTTCATCTAA-3′
	CH-$\alpha1_{CB}$ For	5′-TTATCGTACCTAAATTTAAACACTTATTATAAGCGAACTATA-3′
CH-α2NA	CH-$\alpha2_{NA}$ Rev	5′-GCGTTTTTGAAACGCATCTAAACTTCCAGTAGCTAATTCATT-3′
	CH-$\alpha2_{NA}$ For	5′-GATGCGTTTCAAAAACGCACTATAAAAATTTCAGGTCAAAAC-3′
CH-α2NB	CH-$\alpha2_{NB}$ Rev	5′-GTGCGCAGCTAAAATATCTCGCTTATAATAAGTGTTTAAACT-3′
	CH-$\alpha2_{NB}$ For	5′-GATATTTTAGCTGCGCACCAAAAAGCAATGTATGCTCTTAAG-3′
	*Xba*I For	5′-GCTCTAGAAATAATTTTGTTTAACTTTAAGAAGGAG-3′

[a] Underlined, *Eco*RI restriction site; For, forward; R, reverse.

specifically binds to and inhibits the activity of the C3 convertases on the bacterial surface (21). As such, SCIN prevents phagocytosis following opsonization of *S. aureus* by C3b deposition on its surface. Furthermore, because C5 convertases are no longer formed, SCIN strongly attenuates C5a-induced neutrophil responses and formation of the membrane attack complex (22). Remarkably, SCIN does not enhance dissociation of the C3 convertase as observed for other regulators. In the presence of SCIN large amounts of surface-bound C2a and Bb were found, indicating that SCIN prevents decay acceleration of the C3 convertases. Possibly, this stabilizing effect is part of the mechanism of complement inhibition by SCIN.

Because the C3 convertases initiate all downstream effector functions, modulation of these complexes is highly efficient to inhibit complement (23). SCIN has evolved into a highly specific complement inhibitor acting on the C3 convertases and, for that reason, has a high potential in anti-inflammatory therapy. Given that C3 convertases are localized at the cell surface, low concentrations of the inhibitor may suffice for complete inhibition. Furthermore, SCIN is a soluble and nontoxic molecule, thus, can easily be used as a therapeutic agent. However, due to the presence of preexisting Abs directed to this bacterial exoproduct, SCIN cannot be used in its present form.

A search in the *S. aureus* genome identified three proteins homologous to SCIN: SCIN-B, SCIN-C, and open reading frame (ORF)-D. Characterization of these proteins indicates SCIN-B and C inhibit complement, whereas ORF-D displays no inhibitory activity. Based on the crystal structure presented in this paper we constructed chimeric proteins of SCIN and its nonfunctional homologue ORF-D to identify the active site of SCIN. This information provides insights in convertase modulation by SCIN, and forms a basis for development of small nonimmunogenic convertase inhibitors.

Materials and Methods

Cloning of SCIN and SCIN homologues

DNA sequences encoding the excreted SCIN, SCIN-B, SCIN-C, and ORF-D proteins were amplified by PCR on chromosomal DNA of clinical *S. aureus* strains using primers listed in Table I. *Pfu* Turbo polymerase (Stratagene) was used to create 5′ blunt ends and reverse primers included an *Eco*RI cleavage site downstream of the stop codon. PCR products were digested with *Eco*RI (Invitrogen Life Technologies) and cloned into a prSETB vector (Invitrogen Life Technologies) to enable expression of recombinant proteins with a cleavable N-terminal histidine (His) tag. In this study, we used the prSETB-pshAI vector, a prSETB vector in which the *Bam*HI site was modified into a pshAI site to enable blunt-end cloning of genes directly downstream of the enterokinase cleavage site (24). An extra guanine at the 5′ end of the primers was used to complement the enterokinase cleavage site. The prSETB-pshAI vector was digested with *Eco*RI and pshAI (Westburg) before ligation. Ligation products were transformed into TOP10F′ *Escherichia coli* (Invitrogen Life Technologies) and plasmids of positive clones were analyzed by DNA sequencing. The sequences of

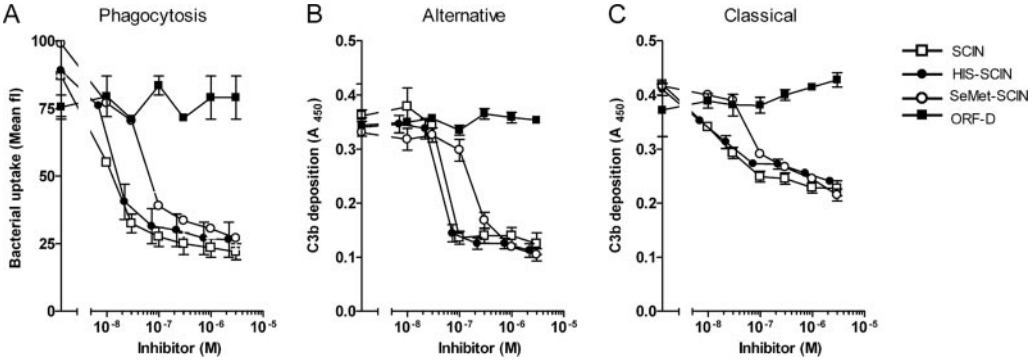

FIGURE 1. Functional analyses of labeled SCIN molecules. Analyses of SCIN, His-tagged SCIN, and selenomethionine-labeled SCIN. *A*, SCIN, His-SCIN, and SeMet-SCIN show a dose-dependent inhibition of *S. aureus* uptake by human neutrophils in 10% human sera. *B*, Dose-dependent inhibition of AP-mediated C3b deposition by SCIN, His-SCIN, and SeMet-SCIN in 30% human serum measured by ELISA. *C*, Dose-dependent inhibition of CP-mediated C3b deposition by SCIN, His-SCIN, and SeMet-SCIN in 5% human serum measured by ELISA. ORF-D was used as a negative control in all three experiments. Data are mean ± SEM of two independent experiments.

cloned genes can be found in the genome databases using the following accession numbers: SCIN (YP_041408/SAR2035 in *S. aureus* MRSA252), SCIN-B (NP_374275, SA1004 in *S. aureus* N315), SCIN-C (YP_040544, SAR1131 in *S. aureus* MRSA252), and ORF-D (YP_039686, SAR0221 in *S. aureus* MRSA252).

Cloning of chimeric proteins

Chimeric proteins of SCIN and ORF-D were constructed by overlap extension PCR (25, 26). *Xba*I-digested SCIN and ORF-D pRSETB vectors were used as templates for amplification of DNA fragments having overlapping ends using complementary primers (Table I) and PCR. For example, to create the SCIN chimera in which the 13 N-terminal residues were replaced with homologous residues of ORF-D, chimera N (CH-N), we designed a sense primer (CH-N forward) and antisense (CH-N reverse) primer containing codon 7–13 of ORF-D combined with codon 14–20 of SCIN. One PCR product was created using pRSETB-ORFD as a template and *Xba*I forward (anneals at the *Xba*I restriction site, upstream of the translation initiation site) and CH-N reverse as primers. Another PCR was performed with pRSETB-SCIN as a template and CH-N forward and SCIN reverse (containing an *Eco*RI site) as primers. The purified PCR products were then diluted, mixed with *Xba*I forward and SCIN reverse primers, and amplified in a third PCR reaction. Because the strands of input PCR products have matching sequences at their 3′ ends, they overlap and act as primers for each other. Simultaneous addition of *Xba*I forward and SCIN reverse resulted in amplification of the full-length PCR product. Some chimeric constructs required the annealing of three PCR products and, therefore, four different primers were designed. All final PCR products spanned from the *Xba*I site on the prSETB vector to the *Eco*RI site at the 3′ end of the gene. Both PCR products and pRSETB vectors were digested with *Xba*I and *Eco*RI before ligation. Ligation products were transformed into TOP10F′ *E. coli* (Invitrogen Life Technologies) and positive clones were analyzed by DNA sequencing.

Protein expression

For expression, recombinant plasmids of both wild-type and chimeric proteins were transformed into *E. coli* Rosetta Gami (DE3) pLysS (Novagen; Merck Biosciences) and expression was conducted according to the manufacturer's instructions. For selenomethionine-labeling of SCIN, pRSETB-SCIN was transformed into strain JG301, a methionine-auxotrophic derivative *E. coli* BL21 Star (DE3) (27). Transformants were grown until mid-exponential phase in minimal medium supplemented with 0.5% (w/v) glucose and 50 μg/ml selenomethionine (27). Expression of selenomethionine-labeled SCIN was performed by incubation with 1 mM isopropyl-1-thio-β-D-galactopyranoside (Roche Applied Science) for 16 h at 37°C. After expression, bacteria were collected by centrifugation and stored at −20°C.

Purification of recombinant proteins

Bacterial pellets were lysed by incubation with 6 M guanidine, 500 mM NaCl, and 20 mM sodium phosphate (pH 7.8) for 30 min at 37°C and subsequent sonication. After centrifugation, His-tagged proteins were purified on a HisTrap nickel column (Amersham Biosciences) which was equilibrated in 8 M urea buffer (containing 1 M NaCl, 10 mM imidazole, and 20 mM sodium phosphate, pH 6). His-tagged SCIN, SCIN-B, SCIN-C, ORF-D, and selenomethionine-SCIN were refolded on the column by gradual lowering urea concentrations during wash steps until the final washing buffer contained 20 mM sodium phosphate, 1 M NaCl, and 10 mM imidazole (pH 6). Refolded proteins were then eluted in 50 mM EDTA in PBS. After dialysis to PBS, the His-tag was cleaved off by a 2-h incubation with enterokinase (3.3 U/ml; Invitrogen Life Technologies) at 37°C. The His-tag was subsequently separated by a second column passage. His-tagged chimeras were not refolded on the column but eluted under denaturing conditions using 0.5 M imidazole in 8 M urea, 1 M NaCl, and 20 mM sodium phosphate (pH 6). Proteins were then refolded by rapid dilution into PBS and subsequently dialyzed against PBS. Because the N-terminal His-tag did not influence SCIN activity (Fig. 1, *A–C*), the tag was not removed for functional screening of chimeric proteins. All recombinant proteins were >95% pure as determined by SDS-PAGE and Coomassie staining. Protein concentrations were assessed by measuring absorbance at 280 nm using the calculated absorbance coefficients.

Crystallization

Purified recombinant selenomethionine-labeled SCIN was dialyzed against 50 mM NaCl and 20 mM Tris (pH 8.0) and concentrated to 24 mg/ml using a Centricon plus-20 filter with a 5-kDa molecular mass cut off (Millipore). Initial crystallization experiments were performed at 20°C by using the sitting drop vapor-diffusion method. A mosquito robot (TTP LabTech) was used to set up 200 nl drops with a 1:1 ratio of protein and reservoir solution. Initial crystals, stacked crystalline plates, were obtained with reservoir solution containing 25% (w/v) PEG 1500, 0.1 M propionic acid-cacodylate bis-tris propane (PCB) buffer, made by mixing 0.1 M sodium propionate, 0.1 M sodium cacodylate, and 0.1 M bis-tris propane in a 2:1:2 ratio at pH 9.0. The initial crystals were reproduced and optimized by hand using 2-μl hanging drops. Large amounts of rectangular plate-like crystals with dimensions 0.2 × 0.1 × 0.08 mm were obtained using reservoir solution consisting of 35% (w/v) PEG 1000 in 0.1 M PCB buffer (pH 8.5). Crystals were harvested from the drops and briefly washed in a 2-μl drop of mother liquor before flash cooling by immersion in liquid nitrogen.

X-ray diffraction and analysis

Diffraction data were collected at ESRF beam-line ID14-EH4 in Grenoble, France. A multiwavelength anomalous dispersion (MAD) data set to a resolution of 1.8 Å was collected using a selenomethionine-labeled SCIN crystal. The data set comprises 400 images in total; 100 images inflection (λ = 0.9795 Å) data, 200 images peak (λ = 0.9793 Å) data, and 100 images remote (λ = 0.9763 Å) data. SCIN crystals displayed the orthorhombic space group $P2_12_12_1$, with unit cell parameters a = 23.02 Å, b = 42.78 Å, and c = 63.91 Å and $\alpha = \beta = \gamma = 90°$. The crystal had a solvent content of 25% with one SCIN molecule per asymmetric unit. Diffraction data were indexed and further processed using the programs MOSFLM (28) and SCALA from the CCP4 program suite, respectively. A summary of the data collection and processing statistics is provided in Table II.

Structure determination and refinement

The structure of SCIN was solved by a three-wavelength (inflection, peak, and remote) selenomethionine MAD experiment with crystals diffracting to

Table II. *Crystallographic data collection and refinement statistics*[a]

Data collection statistics			
Space group	$P2_12_12_1$		
Cell dimensions (Å)	$a = 23.02, b = 42.78, c = 63.91$		
	Peak	Inflection	Remote
Wavelength (Å)	0.9793	0.9795	0.9763
Resolution (Å)	63.9-1.80 (1.90-1.80)	42.8-1.8	64.0-1.80
Completeness (%)	99.9 (100)	99.8 (100)	99.8 (100)
Multiplicity	7.1 (7.4)	3.6 (3.8)	3.6 (3.8)
R_{merge} (%)	6.0 (38.7)	5.2 (38.1)	5.4 (43.9)
I/σI	22.8 (4.3)	16.3 (2.5)	15.4 (2.0)
Refinement statistics			
No. of reflections (work/test)	5952/294		
R/R_{free} (%)	20.1/23.0		
B-factor (Å[a])	21.8		
Root mean square deviation bond length (Å)	0.060		
Root mean square deviation bond angle (°)	0.790		
No. of protein atoms	624		
No. of water molecules	43		

[a] Values between parentheses refer to the highest resolution shell.

1.8 Å resolution. Initial phases were derived from the position of the selenium atoms. One of the two selenium sites was identified with the SOLVE/RESOLVE package (29), whereas no clear solution was obtained for the second selenium site. An initial model was obtained by iterative model-building using RESOLVE (29). This model was completed to ~85% by automated model building using ARP/wARP (30). The model of SCIN was finalized by cycles of model building with COOT (31) and refinement using REFMAC5 (32). Because of radiation damage the automated model building and subsequent iterative refinement was performed using only 200 images of the peak data. The final model has R and R_{free} factors of 20.1 and 22.6%, respectively, and displays good geometry. The model contains 74 protein residues, including 2 selenium methionines, and 43 water molecules. For the side chain of Tyr-53 a double conformation was modeled. Residues 1–8 are missing from the model due to poor electron density, whereas the 3 C-terminal residues (residues 83–85) are not present in the crystal. Coordinates and structure factors have been deposited in the Protein Data Bank (PDB code ID 2QFF). All molecular graphic figures were generated with pymol (W. Delano; http://pymol.sourceforge.net).

Mass spectrometry

The mass of the protein used for crystallization was determined by recording positive-ion MALDI-TOF mass spectra using a Voyager-DE PRO mass spectrometer (Applied Biosystems). SCIN was spotted on a MALDI plate via successive deposition and drying of 1 μl of matrix solution, 1 μl of analyte, and again 1 μl of matrix solution. The matrix and analyte solutions used to prepare these sandwich spots consisted of 10 mg/ml 3,5-dimethoxy-4-hydroxycinnamic acid (sinapinic acid) in water/acetonitrile (1:1) and 1 mg/ml SCIN in 10 mM Tris and 10 mM NaCl (pH 7.5), respectively.

ELISAs

Monoclonal and polyclonal Abs against SCIN were produced and analyzed as described earlier (21, 24). Abs are specific for SCIN because they did not react with SCIN-B, SCIN-C, or ORF-D. mAbs did not react with 15-mer linear peptides spanning the sequence of SCIN, initiating a new peptide every fifth amino acid (Dr. R. van der Zee, Institute of Infectious Diseases and Immunology, Utrecht University, The Netherlands).

Functional activity of complement was screened as described previously (21, 33) with minor modifications. C3b and C5b-9 deposition were detected using anti-C3c WM1 (American Type Culture Collection (34)) and anti-C5b-9 (Abcam) Abs, respectively. Ab binding was detected using peroxidase-conjugated goat anti-mouse IgG (Southern Biotechnology Associates) and visualized using tetramethylbenzidine (35).

Complement activation on S. aureus

Laboratory strain *S. aureus* Cowan EMS was used for phagocytosis and complement activation assays. For phagocytosis experiments, FITC-labeled bacteria were incubated with human sera and freshly isolated human neutrophils for 15 min at 37°C (21). Reactions were stopped in 1% paraformaldehyde and bacterial uptake by 10,000 gated neutrophils was analyzed by flow cytometry. The formation of C5a during opsonization of heat-killed *S. aureus* was measured in a calcium flux assay with fluo-3-acetoxymethyl ester (Molecular Probes) labeled neutrophils (22). Supernatant-induced calcium responses are solely triggered by C5a, because preincubation of neutrophils with the C5a receptor antagonist $CHIPS^{-30}$ (CHIPS, lacking the first 30 N-terminal residues) completely blocked supernatant-induced neutrophil activation (22, 24). The following formula was used to calculate the calcium flux: calcium flux = stimulus-induced fluorescence − background fluorescence. For detection of bacterium-bound Bb and C2a, *S. aureus* Cowan EMS (5×10^6) was incubated with serum for 20 min at 37°C in HEPES buffer (20 mM HEPES, 140 mM NaCl, 5 mM $CaCl_2$, 2.5 mM $MgCl_2$ (pH 7.4), and HBS^{++}), washed and surface-associated proteins were subjected to SDS-PAGE and analyzed by immunoblotting (21). Factor D-deficient serum was prepared by size exclusion chromatography and functionally tested by AP50 (21). Binding of FITC-labeled SCIN (labeled as described for CHIPS (17)) to *S. aureus* was studied by incubation of *S. aureus* Cowan EMS (3×10^7) with 1 μg/ml SCIN-FITC in the presence of nonlabeled SCIN molecules and serum for 20 min. We used 20% factor D-deficient serum in HBS^{++} for analyses of the CP/LP and 20% normal serum in HBS/2 mM $MgCl_2$/2 mM EGTA for the AP. Bacteria were washed and mean fluorescence of 10,000 particles was determined by flow cytometry.

Results

Structure determination

The SCIN protein crystallized in space group $P2_12_12_1$ with one molecule per asymmetric unit and a solvent content of 25%. The structure of SCIN was solved by MAD with data collected from a single selenomethionine-labeled crystal that diffracted to 1.8 Å resolution. The structure of SCIN was refined to an R and R_{free} of 20.1 and 22.6%, respectively, with no outliers in the Ramachandran plot. Poor electron density was observed for the N-terminal region indicating flexibility, accordingly, residues 1–8 were not modeled. In contrast, the C-terminal region is well defined and is involved in multiple crystal contacts. However, no electron density is observed for the three C-terminal residues. MALDI-TOF mass spectrometry analysis of the sample used in the crystallization experiments confirmed the absence of residues 83–85, and consequently, a carboxy terminus was modeled on Lys-82. Absence of residues 83–85 was only found in the concentrated samples (>25 mg/ml) specifically prepared for crystallization experiments. Likely, the three C-terminal residues were cleaved off by the still present and co-concentrated enterokinase used for the removal of the His-tag. Although the activity of SeMet-SCIN was reduced by 5-fold, the specific SCIN activity was retained (Fig. 1, *A–C*). The final model contains 74 residues and 43 water molecules. Data collection and refinement statistics are given in Table II.

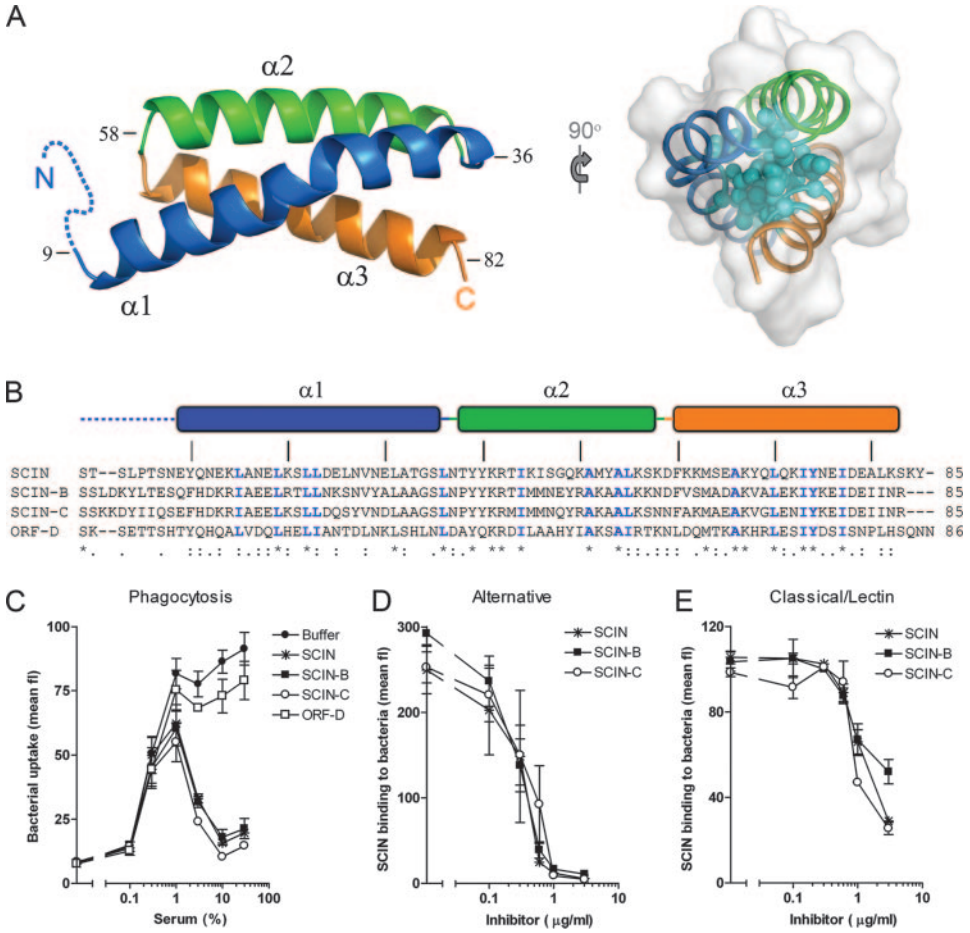

FIGURE 2. Structure of SCIN and characterization of SCIN homologues. *A*, *left panel*, Structure of SCIN shown in ribbon representation. Helices are colored blue (helix 1), green (helix 2), and orange (helix 3), the dotted line represents the flexible N terminus. *A*, *right panel*, SCIN structure in ribbon and surface representation with side chains forming the conserved hydrophobic core in ball-and-stick (light blue) representation, helical coloring as in left panel. *B*, Alignment of SCIN, SCIN B, SCIN C, and ORF-D. *, Identical residues, :, conserved substitutions; ., semiconserved substitutions (CLUSTAL W version 1.83). Highlighted in light blue are the conserved residues that form the hydrophobic core. *C*, SCIN-B and SCIN-C (10 μg/ml) strongly reduce phagocytosis of *S. aureus* at different serum concentrations. ORF-D does not reduce phagocytic uptake. *D* and *E*, Binding of SCIN-FITC (1 μg/ml) to *S. aureus* in 20% human sera in the presence of nonlabeled SCIN, SCIN-B, or SCIN-C. SCIN binding was analyzed by flow cytometry and is expressed as mean fluorescence of 10,000 bacteria. *D*, Nonlabeled SCIN, SCIN-B, and SCIN-C compete with SCIN-FITC for binding to surface-bound C3bBb. Binding to C3bBb was performed in the presence of Mg-EGTA. *E*, Nonlabeled SCIN, SCIN-B, and SCIN-C compete with SCIN-FITC for binding to surface-bound C4b2a. Binding to C4b2a was analyzed using factor D-deficient serum. For all panels, data are mean ± SEM of three independent experiments.

Structure of SCIN

SCIN displays a triple α-helical bundle structure. The three helices are connected via two short loops and adopt a compact arrangement with overall dimensions of ~45 × 25 × 25 Å (Fig. 2*A*). The middle helix, helix α2 (residues Thr-38 to Ser-57), is positioned anti-parallel with respect to both the N- and C-terminal helices α1 (residues Glu-9 to Ser-35) and α3 (residues Phe-60 to Leu-81), respectively. The long helix α1 extends from the N-terminal part of helix 3 to the N-terminal part of helix 2 and is kinked halfway (residues 25–26). The kink distorts the typical α-helical hydrogen bonding pattern and a partial 3_{10}-helix conformation is observed. A second 3_{10}-helix conformation is present at the C-terminal part of helix α1 (Ala-32 to Ser-35). The core of the protein is formed by hydrophobic residues, whereas charged residues face the solvent (Fig. 2*A*). In addition to the hydrophobic interactions, the three helices interact via seven hydrogen bonds and one salt bridge (Glu-18 to Lys-67). Altogether, the structure of SCIN is characterized by three helices packed in a coiled coil.

Identification and characterization of SCIN homologues

In search of structural and functional homologues of SCIN, the Protein Data Bank was screened using the Dali server. This yields >500 proteins from various organisms with very different functions. To the contrary, a Basic Local Alignment Search Tool (BLAST) search in the genome database revealed only a few proteins with homology in sequence. Present in the six available *S. aureus* genomes are the unknown proteins SCIN-B (46% aa identity), SCIN-C (48%), and ORF-D (33%) (Fig. 2*B*). Like SCIN, these proteins have a mass of 9.8 kDa and are excreted via a signal peptide. Secondary structure predictions using the Predict Protein server indicate SCIN-B, SCIN-C, and ORF-D have the same α-helical distribution as present in SCIN. Following recombinant production, analyses of these SCIN homologues show that SCIN-B and SCIN-C are effective complement inhibitors, whereas ORF-D has no complement blocking activity (36). Fig. 2*C* indicates that phagocytosis of fluorescence-labeled *S. aureus* by human neutrophils is strongly inhibited by SCIN, SCIN-B, and SCIN-C (10 μg/ml) at serum concentration of 3% and higher, whereas ORF-D

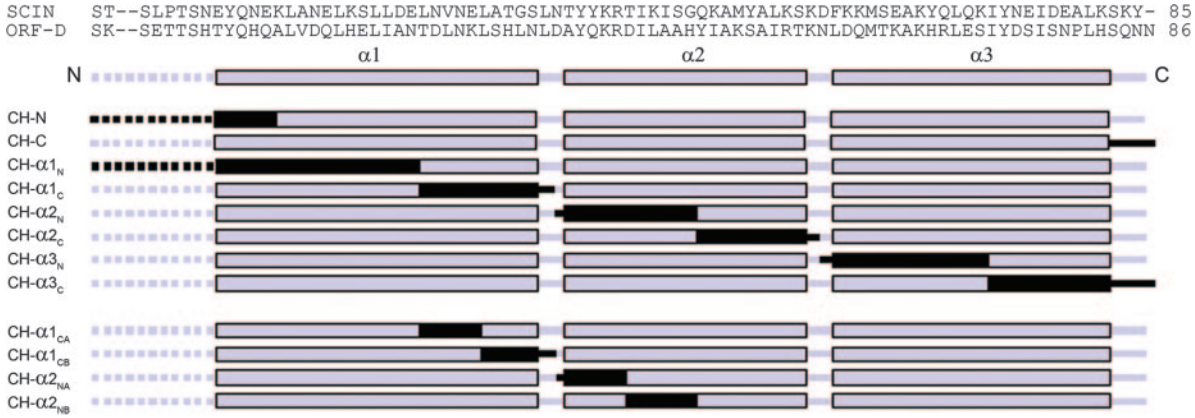

FIGURE 3. Schematic representation of chimeric constructs used in this study. SCIN residues (gray) were exchanged with corresponding residues in ORF-D (black). Exchanged residues: CH-N (residues 1–13), CH-C (residues 83–85), CH-$\alpha1_N$ (residues 1–25), CH-$\alpha1_C$ (residues 26–36), CH-$\alpha2_N$ (residues 37–48), CH-$\alpha2_C$ (residues 49–58), CH-$\alpha3_N$ (residues 59–72), and CH-$\alpha3_C$ (residues 73–86). CH-$\alpha1_{CA}$ (residues 26–30), CH-$\alpha1_{CB}$ (residues 31–36), CH-$\alpha2_{NA}$ (residues 37–42), and CH-$\alpha2_{NB}$ (residues 43–48).

does not inhibit phagocytosis. The remarkable pattern of SCIN inhibition nicely illustrates that the contribution of complement activation to phagocytosis is more pronounced at higher serum concentrations in this assay. Further analyses of SCIN-B and SCIN-C showed they inhibit the complement system similar to SCIN (36). Although SCIN-B is less efficient in inhibition of C3b deposition via the CP and LP, both SCIN homologues block all complement pathways in ELISA. Additionally, SCIN-B and SCIN-C also reduce C4b2a and C3bBb dissociation. To investigate whether the three SCIN molecules bind to similar epitopes, competition-binding experiments were performed. First, we analyzed AP-mediated binding of fluorescence-labeled SCIN (SCIN-FITC) to *S. aureus* in the presence of 10% human serum and Mg-EGTA. Earlier we showed that binding of SCIN to bacterial surfaces occurs when C3bB is activated into C3bBb (21). Fig. 2*D* illustrates that binding of SCIN-FITC (1 μg/ml) to C3bBb is completely blocked in the presence of equal concentrations of nonlabeled SCIN, SCIN-B, or SCIN-C, which indicates that the homologues bind with equal affinity to a similar site within C3bBb. Second, we analyzed CP- and LP-mediated binding of SCIN to *S. aureus* in 10% factor D-deficient serum (to prevent AP activation). SCIN-C prevents binding of SCIN-FITC to C4b2a at identical concentrations as SCIN (Fig. 2*E*). Summarizing, characterization of SCIN and the three SCIN homologues indicates that SCIN-B and C are also convertase inhibitors that bind to similar epitopes on C3bBb. The 33% homologue ORF-D displays no complement inhibitory activity.

Preparation of chimeric proteins

To gain insight into the active site of SCIN, 15-mer linear peptides spanning the molecule (initiating a new peptide every fifth amino acid) were tested for complement inhibitory activity. None of the peptides was active, indicating that the tertiary structure is of importance for SCIN activity. The similarity in m.w. and predicted secondary structure, and the conservation of hydrophobic residues (Fig. 2) forming the protein core indicates that the structures of SCIN and its nonfunctional homologue ORF-D are alike. Based on these observations, eight chimeric proteins (Fig. 3) were designed to localize sites crucial for SCIN function. In chimeras CH-N and CH-C, SCIN residues 1–13 (the flexible N terminus and the first part of helix $\alpha1$) and 83–85 (missing in the structure), respectively, are replaced by homologous residues of ORF-D. In the six other chimeras, half helices are replaced; CH-$\alpha1_N$ (residues 1–25, N-terminal half of helix $\alpha1$ and flexible N terminus), CH-$\alpha1_C$ (residues 26–36, C-terminal half of helix $\alpha1$), CH-$\alpha2_N$ (residues 37–48), CH-$\alpha2_C$ (residues 49–58), CH-$\alpha3_N$ (residues 59–72), and CH-$\alpha3_C$ (residues 73–86). The constructs coding for the chimeric proteins were prepared using the PCR-based overlap extension methodology (25, 26). The proteins were expressed in *E. coli* and purified as His-tagged proteins. The presence of the His-tag does not affect the activity of SCIN (Fig. 1, *A–C*). To demonstrate preservation of secondary structures, we tested binding of 10 different Abs that recognize conformational epitopes of SCIN because they do not react with the 15-mer linear peptides. Each of the chimeras proteins are recognized by multiple Abs indicating the protein structure remained intact (Table III).

SCIN residues 26–48 are crucial for AP inhibition

To determine the residues involved in modulation of the AP, SCIN and the chimeric proteins were tested in an AP-mediated ELISA. Microtiter wells were coated with LPS and incubated with 30%

Table III. *Recognition of chimeric proteins by monoclonal antibodies against SCIN*

	Rabbit	Anti-HIS	2F4	2B12	3G3	3F1	1C9	6C2	6B4	7E3	3G1	1G10
ORF-D		Δ										
SCIN	Δ	Δ	Δ	Δ	Δ	Δ	Δ	Δ	Δ	Δ	Δ	Δ
N	Δ	Δ	Δ	Δ	Δ	Δ	Δ	Δ	Δ	Δ	Δ	Δ
C	Δ	Δ	Δ	Δ	Δ	Δ	Δ	Δ	Δ	Δ	Δ	Δ
$\alpha1_N$	Δ	Δ	Δ	Δ	Δ	Δ	Δ	Δ	Δ	Δ	Δ	
$\alpha1_C$	Δ	Δ		Δ	Δ		Δ		Δ		Δ	
$\alpha2_N$	Δ	Δ			Δ		Δ		Δ		Δ	Δ
$\alpha2_C$	Δ	Δ	Δ	Δ	Δ	Δ	Δ	Δ	Δ		Δ	Δ
$\alpha3_N$	Δ	Δ	Δ	Δ		Δ		Δ		Δ		
$\alpha3_C$	Δ	Δ	Δ	Δ	Δ	Δ	Δ	Δ		Δ	Δ	

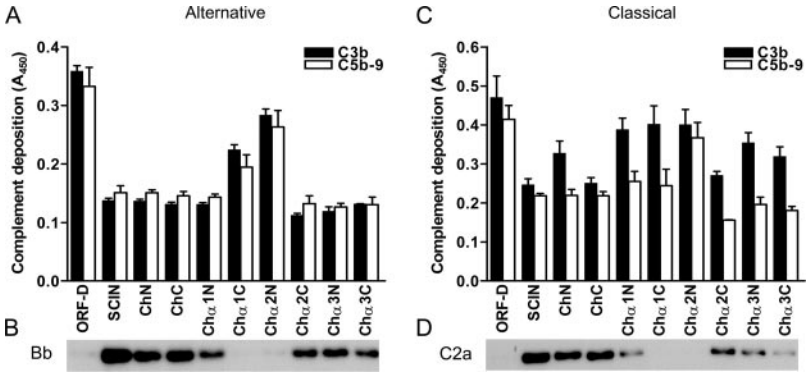

FIGURE 4. SCIN residues 26–48 are crucial for inhibition and stabilization of C3 convertases. *A* and *B*, SCIN residues 26–48 are crucial for inhibition and stabilization of C3bBb. *A*, Effect of chimeric proteins (10^{-6} M) on AP-mediated complement activation in 30% human sera. CH-$\alpha1_C$ and CH-$\alpha2_N$ show reduced complement inhibition, both at the level of C3b and C5b-9 deposition. *B*, CH-$\alpha1_C$ and CH-$\alpha2_N$ do not stabilize C3bBb on bacterial surfaces. Surface detection of Bb on *S. aureus* after opsonization with 20% human serum in the presence of chimeras (10^{-6} M). *C* and *D*, SCIN residues 26–48 are crucial for inhibition and stabilization of C4b2a, but additional domains are required. *C*, Effect of chimeric proteins (10^{-6} M) on CP-mediated complement activation in 5% human sera. C3b deposition was inhibited by SCIN and CH-C, whereas all other chimera had a reduced ability to block C3b deposition. At the level of C5b-9, only CH-$\alpha2_N$ was reduced in its ability to block complement. *D*, CH-$\alpha1_C$ and CH-$\alpha2_N$ do not stabilize C4b2a on bacterial surfaces, whereas other chimeras also show reduced stabilization. Surface detection of C2a on *S. aureus* after opsonization with 20% human serum in the presence of chimeras (10^{-6} M). ELISA data are mean ± SEM of three independent experiments. Blots are a representative of three separate experiments.

human serum in the presence of Mg-EGTA. Subsequently, deposition of C3b and C5b-9 was measured in the presence of SCIN and the chimeras (10 μg/ml). The termini of SCIN are not involved in AP inhibition because chimeric proteins CH-N and CH-C had similar complement inhibitory activities as SCIN (Fig. 4*A*). To the contrary, chimeras CH-$\alpha1_C$ (residues 26–36) and CH-$\alpha2_N$ (residues 37–48) had a markedly reduced capacity to inhibit C3b deposition, whereas inhibition by other chimeras was equal to SCIN. Similarly, C5b-9 formation was inhibited by all chimeras, except by CH-$\alpha1_C$ and CH-$\alpha2_N$. Chimeras from which the N-terminal His-tag was removed by enterokinase inhibited complement in a similar degree, confirming the tag does not alter the functional activity. Previous studies have shown that surface stabilization of the unstable C3 convertases is a hallmark of SCIN activity. To determine the residues involved, the convertase-stabilizing capacity of the chimeras was examined. Following incubation of *S. aureus* with 20% serum in the presence of SCIN and SCIN chimeras (10 μg/ml), surface-bound Bb was detected by immunoblotting. Fig. 4*B* clearly indicates that all chimeras, except for CH-$\alpha1_C$ and CH-$\alpha2_N$, stabilize the AP C3 convertase (C3bBb) formed on the bacterial surface. This implicates that, next to their role in AP inhibition, SCIN residues 26–48 are also crucial for the observed stabilization effect. This indicates, for the first time, that stabilization of surface-bound AP convertase by SCIN is directly linked to inhibition of complement deposition. Taken together, these data indicate that residues 26–48 are crucial for SCIN activity.

Inhibition of CP/LP requires additional regions

To study which residues are involved in inhibition of the CP and LP C3 convertase C4b2a, chimeric proteins were analyzed in a CP ELISA. IgM-coated microtiter wells were incubated with 5% human serum in the presence of SCIN and the chimeras (10 μg/ml) and the deposition of C3b and C5b-9 was monitored. In contrast to the AP, where only two chimeras show reduced complement inhibition, all chimeras, except CH-C, display a reduced ability to prevent C3b deposition in the CP (Fig. 4*C*). This indicates a significant role for regions additional to residues 26–48 in CP inhibition. However, at the level of C5b-9 deposition, only CH-$\alpha2_N$ displays reduced CP inhibition (Fig. 4*C*). In contrast to the AP, we observed different inhibitory patterns for chimeras at the level of C3b and C5b-9, an effect that was also seen at other serum concentrations. This discrepancy might be due to differences in sensitivity of these read-out systems, but we cannot rule out that SCIN inhibition of C3 and C5 convertases in the CP/LP is distinct. As expected, analyses of the chimeric proteins in a LP ELISA revealed similar results (data not shown). To identify SCIN residues involved in stabilization of C4b2a, we determined the amount of C2a molecules at the bacterial surface after opsonization in 20% serum. In correspondence with stabilization of C3bBb, CH-$\alpha1_C$, and CH-$\alpha2_N$ could also not stabilize C4b2a (Fig. 4*D*). However, similar to the observed inhibition of the CP ELISA, other chimeras are also less efficient in stabilizing C4b2a. These data indicate that for the CP/LP additional regions to residues 26–48 are involved in both inhibition of C3b deposition and stabilization of the C3 convertase C4b2a.

Inhibition of C5a responses depends on SCIN residues 26–48

The anaphylatoxin C5a is one of the most potent mediators of inflammation. C5a is formed when C5 is cleaved by the C5 convertase that arises due to high local concentrations of C3b. To determine the residues that inhibit C5a production, SCIN and SCIN chimeras were tested in a system in which all complement pathways are active. *S. aureus* was incubated with 10% human serum in the presence of SCIN chimeras and the supernatants were collected after opsonization. Subsequently, the C5a response of human neutrophils exposed to these supernatants was determined by measuring calcium mobilization (22). The C5a dependency of the supernatant-induced calcium response of neutrophils was verified by preincubation with the C5a receptor antagonist CHIPS $^{-30}$ (24). Fig. 5 indicates that opsonization in the presence of SCIN (10 μg/ml) completely blocks the C5a responses, whereas ORF-D has no effect. Strikingly, the C5a response is not blocked by incubation in presence of chimeras CH-$\alpha1_C$ and CH-$\alpha2_N$, indicating that C5a production is not inhibited. Thus, similar to previously observed in C3b deposition and convertase stabilization, residues 26–48 are also crucial for SCIN-mediated inhibition of C5a formation.

Active site of SCIN pinpointed to 18 residues (31–48)

To further pinpoint the active residues within residues 26–48, we designed four additional chimeras based on CH-$\alpha1_C$ and CH-$\alpha2_N$: CH-$\alpha1_{CA}$ (26–30), CH-$\alpha1_{CB}$ (31–36), CH-$\alpha2_{NA}$ (37–42) and

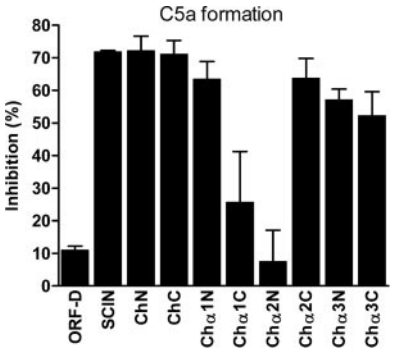

FIGURE 5. SCIN residues 26–48 are crucial for inhibition of C5a responses. CH-$\alpha 1_C$ and CH-$\alpha 2_N$ (10^{-6} M) show a reduced inhibition of C5a-mediated calcium responses. SCIN effectively blocks calcium mobilization of human neutrophils when SCIN is incubated with heat-killed *S. aureus* in 10% human serum to generate C5a-containing supernatants. Supernatant-induced calcium mobilization was measured on fluo-3-AM loaded human neutrophils and determined by flow cytometry. Percentage of inhibition was calculated using the following formula: percentage of inhibition = 100 ((control-induced calcium flux − SCIN-inhibited calcium flux)/control-induced calcium flux). Data are mean ± SEM of three independent experiments.

CH-$\alpha 2_{NB}$ (43–48) (Fig. 3). Structural integrity of these four chimeras was verified by the previously used mAbs that recognize conformational epitopes on SCIN. Chimera CH-$\alpha 1_{CA}$ but not CH-$\alpha 1_{CB}$ blocks C5a responses (Fig. 6*A*). Similarly, CH-$\alpha 1_{CA}$ stabilized C4b2a and C3bBb on the bacterial surface, whereas CH-$\alpha 1_{CB}$ does not affect convertase stability (Fig. 6*B*). The fact that CH-$\alpha 1_{CA}$ blocks complement while CH-$\alpha 1_{CB}$ is not active indicates that residues 26–30 are not involved in SCIN activity. For residues 37–48 we could not pinpoint the activity to a smaller region; CH-$\alpha 2_N$ lacks inhibitory activity whereas the smaller chimeras, CH-$\alpha 2_{NA}$ and CH-$\alpha 2_{NB}$, both inhibit the C5a response and stabilize surface bound convertases (Fig. 6). Altogether, a stretch of 18 residues (31–48) is identified that is crucial in SCIN-mediated complement inhibition.

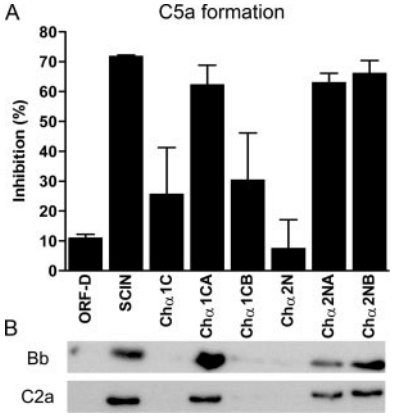

FIGURE 6. SCIN residues 31–48 are crucial for complement inhibition and stabilization of C3 convertases. *A*, CH-$\alpha 1_{CA}$, CH-$\alpha 2_{NA}$, and CH-$\alpha 2_{NB}$ show a reduced inhibition of C5a-mediated calcium responses. CH-$\alpha 1_{CB}$ could not block C5a responses. Data are mean ± SEM of three independent experiments. *B*, CH-$\alpha 1_{CA}$, CH-$\alpha 2_{NA}$, and CH-$\alpha 2_{NB}$ stabilize C3bBb and C4b2a on bacterial surfaces, whereas CH-$\alpha 1_{CB}$ did not stabilize C3 convertases. Blot is a representative of three separate experiments. Proteins were tested at 10^{-6} M.

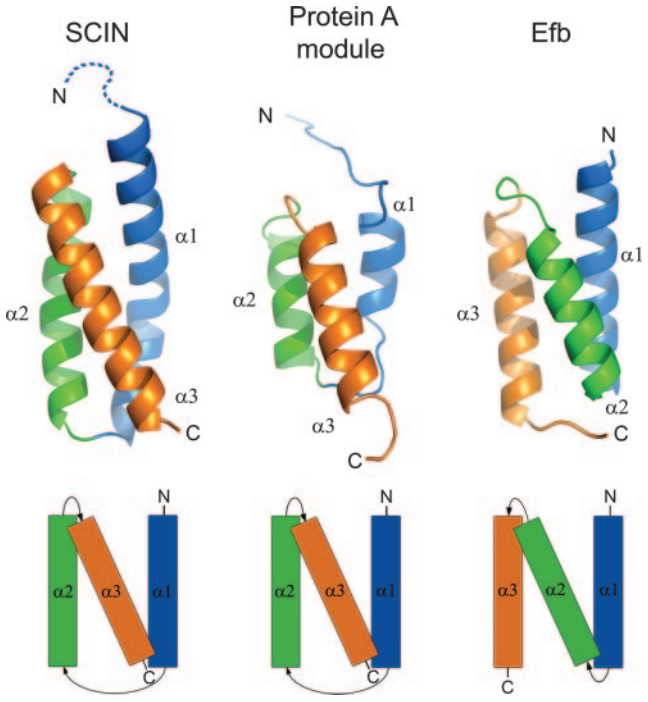

FIGURE 7. Structural comparison of three *S. aureus* immune modulators. SCIN (*left panel*), protein A module (*middle panel*, pdb 1bdd), and Efb-C (*right panel*, pdb 2gom) in ribbon and schematic representation. Helices are colored blue (helix 1), green (helix 2), and orange (helix 3).

Discussion

Ninety percent of *S. aureus* strains express SCIN, an important factor in the staphylococcal defense against the human innate immune system. SCIN is a regulator of C3 convertases that, already at a low concentration, strongly prevents inflammatory reactions evoked by complement. Convertase regulation by SCIN differs significantly from other described convertase regulators. The human regulators of complement activation (RCA) are cell-bound or fluid-phase proteins that protect cells from excessive complement activation by down-regulation of the convertases. Most RCA proteins both promote dissociation of already formed convertases and inhibit formation of new convertases (37). The RCA family includes relatively large proteins that primarily consist of tandem repeats of complement control protein domains that adopt a typical β-sandwich fold stabilized by pairs of disulfide bonds. Several bacteria protect themselves from complement eradication by attracting RCA proteins to their surface (38–40). Viruses have copied genetic material and express RCA-like molecules on virus-infected cells (41, 42). SCIN is a small *S. aureus* convertase inhibitor that functions in a completely different way. SCIN exclusively binds to the activated complex and does not bind individual convertase components (21). SCIN binding increases convertase stability, a remarkable property that, in this study, was shown to be crucial for SCIN activity. The crystal structure of SCIN reveals an all-helical protein with a flexible N terminus. The SCIN fold deviates significantly from other convertase regulators, indicating SCIN belongs to a new class of convertase inhibitors.

Next to SCIN, *S. aureus* produces two SCIN homologues that function in a similar way. In the majority of clinical strains, we find coexpression of either SCIN-B or SCIN-C in combination with SCIN. All SCIN molecules are human-specific, produced in vivo, and expressed simultaneously during bacterial growth. Why *S. aureus* encodes three convertase inhibitors that bind the same epitope on C3bBb remains an intriguing question. Certainly, it

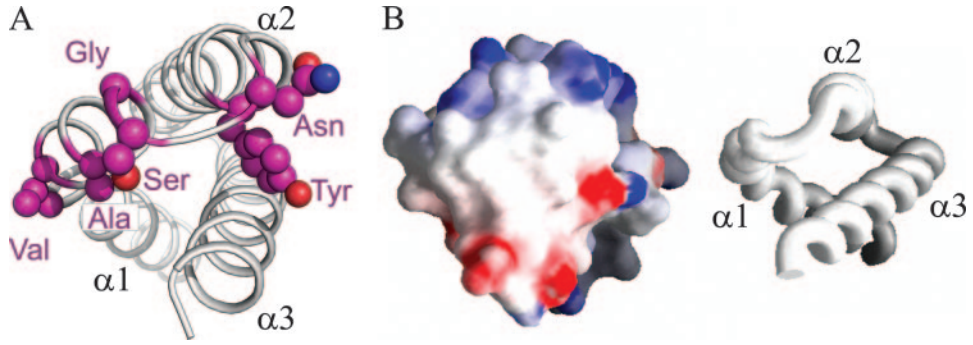

FIGURE 8. Active site residues of SCIN for the AP. *A*, SCIN show in ribbon representation (gray) with active site residues conserved within SCIN, SCIN-B, and SCIN-C but not in ORF-D highlighted and shown in ball-and-stick representation (purple). *B*, *left panel*, Electrostatic surface representation in and around the SCIN active site. Positively charged regions are represented in blue, negatively charged regions in red, and both polar and nonpolar regions are in white. *Right panel*, Similar view of SCIN shown in ribbon representation. Pictures were generated by GRASP (47).

illustrates that convertase modulation strongly contributes to the organism's ability to infect humans.

The compact all-helical structure of SCIN indicates a new mechanism for convertase inhibition. Recent structural determination of the C3-binding domain of Efb (Efb-C) from *S. aureus* revealed this is an all-helical protein as well (43). We have recently discovered that this C3/C3b-binding protein also regulates surface-bound convertases (36). By binding to C3b, Efb-C blocks substrate cleavage of the convertases that harbor a C3b molecule (AP C3 convertase and all C5 convertases). In contrast to SCIN, Efb-C does not stabilize convertases and directly binds isolated C3b. Comparison of the SCIN and Efb-C structures reveals that the topological arrangement of the three helices differs significantly (Fig. 7). Although SCIN does not directly bind isolated C3b, it is possible that SCIN does bind to C3b molecules in the context of the convertase complex. Because SCIN inhibits both the AP convertase (C3bBb) and the CP/LP convertase (C4b2a), putative binding to C3/C3b indicates a mechanism in which SCIN interacts with the substrate C3. Alternatively, direct binding to activated C2 and factor B, which provide the catalytic center to the C3 convertase (44, 45), could explain the inhibitory activity of SCIN. In such a model, SCIN would lock the convertase catalytic center in an inactive conformation and/or block substrate binding. However, residues Leu-26 to Gly-48, essential for the inhibiting activity of SCIN, adopt a distinct helix-loop-helix conformation that deviates significantly from the large and flexible inhibitory loops observed in trypsin inhibitors. The absence of SCIN affinity toward the isolated components of the convertases indicates specific conformations within the convertase are pivotal for SCIN binding.

Within the active helix-loop-helix segment, six residues (28-VxxxAxGSxNxxY-40) are conserved among the three active SCIN molecules and are absent in the structural but nonfunctional homologue ORF-D (Fig. 8). In the structure of SCIN these residues are positioned on opposite sides which may indicate SCIN binds via two sides to the convertase. The six residues are positioned in a noncharged plane that is sandwiched by the positively and negatively charged top and bottom sides of SCIN, respectively. Due to the relative small size, SCIN could easily fit into a pocket of one of the much larger convertase components. A two binding site model agrees with the observation that SCIN binding stabilizes the convertase. A comparable cross-linking is proposed for a single *S. aureus* protein A domain that, despite its small size (~7 kDa), simultaneously can bind the Fc and the Fab region of immunoglobulins (46). Interestingly, comparison of SCIN with the five extracellular Ig-binding modules of the *S. aureus* protein A reveals a striking similarity in helical arrangement (Fig. 7). In summary, the capacity to stabilize the convertase and the opposite orientation of conserved residues within the active site may indicate SCIN binds to both components of the C3 convertase.

With the current lack of proper treatment for complement-mediated diseases, insights into the specific and effective complement inhibition by SCIN provide a useful tool in the development of a nonimmunogenic complement inhibitor. Due to preexisting Abs, generation of a smaller compound with complement inhibitory capacity will be crucial for therapeutic use of SCIN. To pinpoint residues that are an absolute requirement for a small-molecule derivative of SCIN, we have identified the most active regions in the protein. To establish this, the chimeric proteins were analyzed at concentrations of 10^{-6} M. There, a loss in activity represents a >100-fold reduced function (Fig. 1). At low inhibitor concentrations, less important regions could be highlighted (for example, the regions mutated in the SeMet-labeled SCIN lacking aa 83–85), but because these mutants exert all specific SCIN functions (convertase stabilization and complement inhibition) at higher protein concentrations, we do not consider these sites to be essential for SCIN activity. The fact that critical sites for modulation of the AP are located in a distinct part (Leu-26 to Gly-48) of SCIN is promising for development of a small complement inhibitory compound. The same stretch of residues was shown to be critical in assays in which all complement initiation routes were triggered and C5a response was analyzed. The structure and the identification of the active site of SCIN presented in this paper provide a starting point for structure-based drug design.

Acknowledgments

We acknowledge the European Synchrotron Radiation Facility for provision of synchrotron radiation facilities and we thank the beamline scientists at ID-14-EH4 for help with data collection. We thank Jeroen Geurtsen for providing the methionine-auxotrophic *E. coli* strain.

Disclosures

The authors have no financial conflict of interest.

References

1. Walport, M. J. 2001. Complement: second of two parts. *N. Engl. J. Med.* 344: 1140–1144.
2. Walport, M. J. 2001. Complement: first of two parts. *N. Engl. J. Med.* 344: 1058–1066.
3. Carroll, M. C. 2004. The complement system in regulation of adaptive immunity. *Nat. Immunol.* 5: 981–986.
4. Seelen, M. A., A. Roos, and M. R. Daha. 2005. Role of complement in innate and autoimmunity. *J. Nephrol.* 18: 642–653.
5. Trouw, L. A., M. A. Seelen, and M. R. Daha. 2003. Complement and renal disease. *Mol. Immunol.* 40: 125–134.
6. Fujita, T., M. Matsushita, and Y. Endo. 2004. The lectin-complement pathway: its role in innate immunity and evolution. *Immunol. Rev.* 198: 185–202.

7. Xu, Y., S. V. Narayana, and J. E. Volanakis. 2001. Structural biology of the alternative pathway convertase. *Immunol. Rev.* 180: 123–135.
8. Lambris, J. D. 1988. The multifunctional role of C3, the third component of complement. *Immunol. Today* 9: 387–393.
9. Janssen, B. J., A. Christodoulidou, A. McCarthy, J. D. Lambris, and P. Gros. 2006. Structure of C3b reveals conformational changes that underlie complement activity. *Nature* 444: 213–216.
10. Janssen, B. J., E. G. Huizinga, H. C. Raaijmakers, A. Roos, M. R. Daha, K. Nilsson-Ekdahl, B. Nilsson, and P. Gros. 2005. Structures of complement component C3 provide insights into the function and evolution of immunity. *Nature* 437: 505–511.
11. Helmy, K. Y., K. J. Katschke, Jr., N. N. Gorgani, N. M. Kljavin, J. M. Elliott, L. Diehl, S. J. Scales, N. Ghilardi, and C. M. van Lookeren. 2006. CRIg: a macrophage complement receptor required for phagocytosis of circulating pathogens. *Cell* 124: 915–927.
12. Gasque, P. 2004. Complement: a unique innate immune sensor for danger signals. *Mol. Immunol.* 41: 1089–1098.
13. Pangburn, M. K., and N. Rawal. 2002. Structure and function of complement C5 convertase enzymes. *Biochem. Soc. Trans.* 30: 1006–1010.
14. Foster, T. J. 2005. Immune evasion by staphylococci. *Nat. Rev. Microbiol.* 3: 948–958.
15. Rooijakkers, S. H., K. P. van Kessel, and J. A. van Strijp. 2005. Staphylococcal innate immune evasion. *Trends Microbiol.* 13: 596–601.
16. Bestebroer, J., M. J. Poppelier, L. H. Ulfman, P. J. Lenting, C. V. Denis, K. P. van Kessel, J. A. van Strijp, and C. J. de Haas. 2006. Staphylococcal superantigen-like 5 binds PSGL-1 and inhibits P-selectin-mediated neutrophil rolling. *Blood* 109: 2936–2943.
17. de Haas, C. J., K. E. Veldkamp, A. Peschel, F. Weerkamp, W. J. van Wamel, E. C. Heezius, M. J. Poppelier, K. P. van Kessel, and J. A. van Strijp. 2004. Chemotaxis inhibitory protein of *Staphylococcus aureus*, a bacterial anti-inflammatory agent. *J. Exp. Med.* 199: 687–695.
18. Postma, B., M. J. Poppelier, J. C. van Galen, E. R. Prossnitz, J. A. van Strijp, C. J. de Haas, and K. P. van Kessel. 2004. Chemotaxis inhibitory protein of *Staphylococcus aureus* binds specifically to the C5a and formylated peptide receptor. *J. Immunol.* 172: 6994–7001.
19. Lee, L. Y., X. Liang, M. Hook, and E. L. Brown. 2004. Identification and characterization of the C3 binding domain of the *Staphylococcus aureus* extracellular fibrinogen-binding protein (Efb). *J. Biol. Chem.* 279: 50710–50716.
20. Langley, R., B. Wines, N. Willoughby, I. Basu, T. Proft, and J. D. Fraser. 2005. The staphylococcal superantigen-like protein 7 binds IgA and complement C5 and inhibits IgA-FcαRI binding and serum killing of bacteria. *J. Immunol.* 174: 2926–2933.
21. Rooijakkers, S. H., M. Ruyken, A. Roos, M. R. Daha, J. S. Presanis, R. B. Sim, W. J. van Wamel, K. P. van Kessel, and J. A. van Strijp. 2005. Immune evasion by a staphylococcal complement inhibitor that acts on C3 convertases. *Nat. Immunol.* 6: 920–927.
22. Rooijakkers, S. H., M. Ruyken, J. van Roon, K. P. van Kessel, J. A. van Strijp, and W. J. van Wamel. 2006. Early expression of SCIN and CHIPS drives instant immune evasion by *Staphylococcus aureus*. *Cell. Microbiol.* 8: 1282–1293.
23. Wang, Y. 2006. Complementary therapies for inflammation. *Nat. Biotechnol.* 24: 1224–1226.
24. Haas, P. J., C. J. de Haas, W. Kleibeuker, M. J. Poppelier, K. P. van Kessel, J. A. Kruijtzer, R. M. Liskamp, and J. A. van Strijp. 2004. N-terminal residues of the chemotaxis inhibitory protein of *Staphylococcus aureus* are essential for blocking formylated peptide receptor but not C5a receptor. *J. Immunol.* 173: 5704–5711.
25. Postma, B., W. Kleibeuker, M. J. Poppelier, M. Boonstra, K. P. van Kessel, J. A. van Strijp, and C. J. de Haas. 2005. Residues 10–18 within the C5a receptor N terminus compose a binding domain for chemotaxis inhibitory protein of *Staphylococcus aureus*. *J. Biol. Chem.* 280: 2020–2027.
26. Ho, S. N., H. D. Hunt, R. M. Horton, J. K. Pullen, and L. R. Pease. 1989. Site-directed mutagenesis by overlap extension using the polymerase chain reaction. *Gene* 77: 51–59.
27. Rutten, L., J. Geurtsen, W. Lambert, J. J. Smolenaers, A. M. Bonvin, A. de Haan, P. van der Ley, M. R. Egmond, P. Gros, and J. Tommassen. 2006. Crystal structure and catalytic mechanism of the LPS 3-O-deacylase PagL from *Pseudomonas aeruginosa*. *Proc. Natl. Acad. Sci. USA* 103: 7071–7076.
28. Leslie, A. G. 2006. The integration of macromolecular diffraction data. *Acta Crystallogr. D* 62: 48–57.
29. Terwilliger, T. C. 2003. Automated main-chain model building by template matching and iterative fragment extension. *Acta Crystallogr. D* 59: 38–44.
30. Perrakis, A., R. Morris, and V. S. Lamzin. 1999. Automated protein model building combined with iterative structure refinement. *Nat. Struct. Biol.* 6: 458–463.
31. Emsley, P., and K. Cowtan. 2004. Coot: model-building tools for molecular graphics. *Acta Crystallogr. D* 60: 2126–2132.
32. Winn, M. D., M. N. Isupov, and G. N. Murshudov. 2001. Use of TLS parameters to model anisotropic displacements in macromolecular refinement. *Acta Crystallogr. D* 57: 122–133.
33. Roos, A., L. H. Bouwman, J. Munoz, T. Zuiverloon, M. C. Faber-Krol, Fallaux-van den Houten, F. C., N. Klar-Mohamad, C. E. Hack, M. G. Tilanus, and M. R. Daha. 2003. Functional characterization of the lectin pathway of complement in human serum. *Mol. Immunol.* 39: 655–668.
34. Veldkamp, K. E., K. P. van Kessel, J. Verhoef, and J. A. van Strijp. 1997. Staphylococcal culture supernates stimulate human phagocytes. *Inflammation* 21: 541–551.
35. Rooijakkers, S. H., W. J. van Wamel, M. Ruyken, K. P. van Kessel, and J. A. van Strijp. 2005. Anti-opsonic properties of staphylokinase. *Microbes Infect.* 7: 476–484.
36. Jongerius, I., J. Köhl, M. K. Pandey, M. Ruyken, K. P. van Kessel, J. A. van Strijp, and S. H. Rooijakkers. 2007. Staphylococcal complement evasion by various convertase-blocking molecules. *J. Exp. Med.* In press.
37. Kirkitadze, M. D., and P. N. Barlow. 2001. Structure and flexibility of the multiple domain proteins that regulate complement activation. *Immunol. Rev.* 180: 146–161.
38. Jarva, H., T. S. Jokiranta, R. Wurzner, and S. Meri. 2003. Complement resistance mechanisms of streptococci. *Mol. Immunol.* 40: 95–107.
39. Ram, S., M. Cullinane, A. M. Blom, S. Gulati, D. P. McQuillen, B. G. Monks, C. O'Connell, R. Boden, C. Elkins, M. K. Pangburn, et al. 2001. Binding of C4b-binding protein to porin: a molecular mechanism of serum resistance of *Neisseria gonorrhoeae*. *J. Exp. Med.* 193: 281–295.
40. Kraiczy, P., J. Hellwage, C. Skerka, M. Kirschfink, V. Brade, P. F. Zipfel, and R. Wallich. 2003. Immune evasion of *Borrelia burgdorferi*: mapping of a complementinhibitor factor H-binding site of BbCRASP-3, a novel member of the Erp protein family. *Eur. J. Immunol.* 33: 697–707.
41. Finlay, B. B., and G. McFadden. 2006. Anti-immunology: evasion of the host immune system by bacterial and viral pathogens. *Cell* 124: 767–782.
42. Mullick, J., J. Bernet, Y. Panse, S. Hallihosur, A. K. Singh, and A. Sahu. 2005. Identification of complement regulatory domains in vaccinia virus complement control protein. *J. Virol.* 79: 12382–12393.
43. Hammel, M., G. Sfyroera, D. Ricklin, P. Magotti, J. D. Lambris, and B. V. Geisbrecht. 2007. A structural basis for complement inhibition by *Staphylococcus aureus*. *Nat. Immunol.* 8: 430–437.
44. Milder, F. J., L. Gomes, A. Schouten, B. J. Janssen, E. G. Huizinga, R. A. Romijn, W. Hemrika, A. Roos, M. R. Daha, and P. Gros. 2007. Factor B structure provides insights into activation of the central protease of the complement system. *Nat. Struct. Mol. Biol.* 14: 224–228.
45. Milder, F. J., H. C. Raaijmakers, M. D. Vandeputte, A. Schouten, E. G. Huizinga, R. A. Romijn, W. Hemrika, A. Roos, M. R. Daha, and P. Gros. 2006. Structure of complement component C2A: implications for convertase formation and substrate binding. *Structure* 14: 1587–1597.
46. Graille, M., E. A. Stura, A. L. Corper, B. J. Sutton, M. J. Taussig, J. B. Charbonnier, and G. J. Silverman. 2000. Crystal structure of a *Staphylococcus aureus* protein A domain complexed with the Fab fragment of a human IgM antibody: structural basis for recognition of B-cell receptors and superantigen activity. *Proc. Natl. Acad. Sci. USA* 97: 5399–5404.
47. Nicholls, A., K. A. Sharp, and B. Honig. 1991. Protein folding and association: insights from the interfacial and thermodynamic properties of hydrocarbons. *Proteins* 11: 281–296.